JOURNAL OF AGRICULTURAL AND FOOD CHEMISTRY

Article

pubs.acs.org/JAFC

Construction of a Green Fluorescent Protein (GFP)-Marked Multifunctional Pesticide-Degrading Bacterium for Simultaneous Degradation of Organophosphates and γ-Hexachlorocyclohexane

Chao Yang,[†,∥] Ruihua Liu,[‡,∥] Yulan Yuan,[§] Jianli Liu,[⊥] Xiangyu Cao,*[,⊥] Chuanling Qiao,[§] and Cunjiang Song*[,†]

[†]Key Laboratory of Molecular Microbiology and Technology for Ministry of Education, Nankai University, Tianjin 300071, China

[‡]State Key Laboratory of Medicinal Chemical Biology and College of Pharmacy, Nankai University, Tianjin 300071, China

[§]State Key Laboratory of Integrated Management of Pest Insects and Rodents, Institute of Zoology, Chinese Academy of Sciences, Beijing 100101, China

[⊥]School of Life Science, Liaoning University, Shenyang 110036, China

ABSTRACT: An autofluorescent whole-cell biocatalyst capable of simultaneously degrading organophosphates (OPs) and γ-hexachlorocyclohexane (γ-HCH) was constructed by display of organophosphorus hydrolase (OPH) and green fluorescent protein (GFP) fusion on the cell surface of a γ-HCH-degrading *Sphingobium japonicum* UT26 using the truncated ice nucleation protein (INPNC) as an anchoring motif. The surface localization of INPNC−OPH−GFP fusion was verified by cell fractionation, Western blot, proteinase accessibility, and immunofluorescence microscopy. Surface display of macromolecular OPH−GFP fusion (63 kDa) neither inhibits cell growth nor affects cell viability. In sterile and nonsterile soil samples, a mixture of parathion (100 mg kg^{-1}) and γ-HCH (10 mg kg^{-1}) could be degraded completely within 15 days when inoculated with the engineered UT26, and the strain could be easily monitored by fluorescence during bioremediation. These results indicate that the engineered UT26 is a promising multifunctional bacterium that could be used for the bioremediation of environments contaminated with multiple pesticides.

KEYWORDS: *cell surface display, organophosphorus hydrolase, green fluorescent protein, γ-hexachlorocyclohexane, Sphingobium japonicum UT26*

INTRODUCTION

Over the past few decades, there has been an increased use of pesticides in agriculture, industry, and residential settings all over the world. As a result of excessive and continuous use, many terrestrial and aquatic ecosystems across the world are contaminated with pesticides. For instance, the output of pesticides in China reached approximately 1.74 million tons of 300 different types of pesticides in 2008, which has made China the largest producer and user of pesticides in the world.[1]

More than 100 organophosphate (OP) pesticides are in use worldwide, accounting for ∼38% of total pesticide usage. In the United States alone, approximately 50000 tons of OP pesticides are used per year.[2] OP compounds are highly toxic to mammals, including humans. Approximately 3 million poisonings and 300,000 human deaths occur per year owing to OP ingestion, and OP poisoning is a global clinical problem.[3] OPs are acute neurotoxins by virtue of their potent inhibition of acetylcholinesterase.[4]

Organophosphorus hydrolase (OPH), isolated from natural soil microorganisms *Pseudomonas diminuta* MG and *Flavobacterium* sp. strain ATCC 27551, can hydrolyze various OP pesticides containing P−O, P−F, and P−S bonds.[2] Hydrolysis of OPs by OPH reduces their toxicity by several orders of magnitude, providing a promising enzymatic detoxification technology.[4] Practical applications of large-scale enzymatic degradation have always been limited by the cost of purification and stability of OPH. In the case of whole cells, the outer membrane acting as a permeability barrier prevents OPs from interacting with OPH residing within the cell.[5] To overcome the potential substrate uptake limitation, various surface-anchoring motifs have been used to target the OPH onto the cell surface, including the Lpp-OmpA chimera, ice nucleation protein (INP), and autotransporter.[5−7] The INP, which nucleates ice formation in supercooled water, has a multidomain organization with an N-terminal domain containing three or four transmembrane spans, a C-terminal domain, and a highly repetitive central domain for ice nucleation.[8,9] It has been demonstrated that truncated INP derivatives serve as anchoring motifs to target foreign proteins onto the cell surface.[6,10]

γ-Hexachlorocyclohexane (γ-HCH) is a highly chlorinated pesticide that causes serious environmental problems due to its toxicity and long persistence in upland soils.[11] Technical HCH (t-HCH) mainly consists of α-, β-, γ-, and δ-isomers. Among these four isomers, only γ-HCH (also called lindane) has insecticidal activity. China had been a major producer and consumer of t-HCH from the 1950s until the government imposed restrictions on its production and agricultural use in

Received: November 21, 2012
Revised: January 16, 2013
Accepted: January 22, 2013
Published: January 22, 2013

1983. In a 30 year period, total production of t-HCH (4.9 million tons) in China accounted for one-third of the global total production.[12] Even after the prohibition of t-HCH, 3200 tons of lindane was still used in forest management between 1991 and 2000.[13]

Many γ-HCH-degrading bacteria such as *Sphingobium japonicum* UT26 from Japan,[14] *Sphingobium indicum* B90 from India,[15] and *Sphingobium francense* Sp+ from France[16] have been isolated and characterized. *S. japonicum* UT26 was isolated from an upland experimental field to which γ-HCH had been applied once a year for 12 years.[17] UT26 utilizes γ-HCH as a sole source of carbon and energy under aerobic conditions. The degradation pathway of γ-HCH was extensively analyzed in *Sphingobium paucimobilis* UT26. In UT26, γ-HCH is converted to β-ketoadipate via sequential reactions catalyzed by LinA (dehydrochlorinase) to LinF (maleylacetate reductase), and β-ketoadipate is further metabolized in the TCA cycle.[11,18]

Bioremediation, which involves the use of microorganisms to detoxify and degrade environmental contaminants, has received considerable attention as an effective biotechnological approach to clean up polluted environments.[18] To date, wild-type microbes that simultaneously degrade OPs and γ-HCH have not been isolated from the environment. Because agricultural soils are usually contaminated with multiple pesticides, multifunctional genetically engineered microorganisms (GEMs) with the capability to degrade various kinds of pesticides are needed to clean up these pesticide residues.

Stable marker systems are required for monitoring the fate and activity of the engineered microbes released into the environment. The green fluorescent protein (GFP), a unique marker that can be detected by noninvasive methods, requires no cofactors or exogenous substrates for its fluorescence.[19] Moreover, GFP can be expressed as either an N- or a C-terminal fusion and still fluoresces. Enhanced GFP, which is a red-shifted variant of GFP, assembles the chromophore more rapidly, shows much stronger fluorescence than wild-type GFP, and fluoresces after exposure to daylight.[20]

In this study, we used the INP anchoring motif for the functional display of the OPH−GFP fusion on the cell surface of a natural γ-HCH-degrading bacterium, *S. japonicum* UT26. The engineered strain was endowed with the capability to simultaneously degrade OPs and γ-HCH, and it could potentially be tracked by fluorescence during bioremediation.

MATERIALS AND METHODS

Bacterial Strains, Plasmids, and Culture Conditions. *S. japonicum* UT26 was grown on 1/3 Luria−Bertani (LB) medium[21] or minimal salts medium (MSM)[22] supplemented with kanamycin to a final concentration of 50 μg/mL. A surface expression vector, pNOG33,[23] coding for INPNC−OPH−GFP fusion was used to target the OPH−GFP fusion onto the cell surface. An expression vector, pOG33,[23] coding for OPH−GFP fusion was used as a control. All chemicals used in this study were purchased from Sigma.

Transformation of plasmids into *S. japonicum* UT26 was performed using the electroporation method of Grag et al.[24] Expression of INPNC−OPH−GFP fusion was induced with 0.2 mM isopropyl-β-D-thiogalactopyranoside (IPTG) for 24 h at 30 °C when cells were grown to an optical density at 600 nm (OD_{600}) of 0.4.

Cell Fractionation. Cells were harvested and resuspended in 25 mM Tris-HCl buffer (pH 8.0). After disruption of the cells by sonication and a brief clarifying spin, the clarified lysate was ultracentrifuged at 50000 rpm for 1 h at 4 °C, and the supernatant was retained as the soluble fraction. The pellet (total membrane fraction) was resuspended with PBS containing 0.01 mM $MgCl_2$ and 2% Triton X-100 for solubilizing the inner membrane and was incubated for 30 min at room temperature, and then the outer membrane fraction was repelleted by ultracentrifugation.[22]

SDS-PAGE and Western Blot Analysis. Samples of different subcellular fractions were mixed with sample buffer (200 mM Tris-HCl, pH 6.8, 8% SDS, 0.04% bromophenol blue, 8% β-mercaptoethanol, 40% glycerol), boiled for 5 min, and analyzed by 12% SDS-PAGE.[21] After electrophoresis, the separated proteins were electroblotted overnight at 40 V to the nitrocellulose membrane (Millipore) with a tank transfer system (Bio-Rad) containing a transfer buffer (25 mM Tris, 192 mM glycine, 10% methanol). After nonspecific binding sites had been blocked with 3% bovine serum albumin (BSA) in TBST buffer (20 mM Tris-HCl, pH 7.5, 150 mM NaCl, 0.05% Tween-20), the membrane was incubated with rabbit anti-GFP polyclonal antibody at a 1:1000 dilution in TBST buffer for 3 h. Subsequently, the membrane was incubated with alkaline phosphatase-conjugated goat anti-rabbit IgG secondary antibody (Promega) at a 1:2000 dilution in TBST buffer for 2 h. The membrane was then stained with nitro blue tetrazolium−BCIP (5-bromo-4-chloro-3-indolylphosphate) in alkaline phosphatase buffer (100 mM Tris-HCl, pH 9.0, 100 mM NaCl) for visualization of antigen−antibody conjugates.

Immunofluorescence Microscopy. Cells were harvested and resuspended (OD_{600} = 0.5) in PBS with 3% BSA. Cells were then incubated with rabbit anti-GFP polyclonal antibody diluted (1:500) in PBS for 3 h at 30 °C. After being washed with PBS, the cells were resuspended in PBS with goat anti-rabbit IgG antibody conjugated with rhodamine (1:100 dilution, Invitrogen) and incubated for 2 h at 30 °C. Prior to microscopic observation, cells were washed five times with PBS and mounted on poly(L-lysine)-coated microscopic slides. Photographs were taken using a fluorescence microscope (Nikon) equipped with FITC and rhodamine filters.

OPH Activity Assay. OPH activity was assayed with paraoxon by monitoring the increases in the absorbance at 405 nm (ε_{405} = 17700 M^{-1} cm^{-1} for *p*-nitrophenol) for 2 min at 37 °C using a Beckman DU800 spectrophotometer.[5] For each assay, 200 μL of cells (OD_{600} = 1.0) was added to 700 μL of 50 mM citrate−phosphate buffer with 50 μM $CoCl_2$ (pH 8.0) and 100 μL of 20 mM paraoxon (Sigma) in 10% methanol. Activities are expressed as units (1 μmol of *p*-nitrophenol produced per minute) per OD_{600} of whole cells.

Fluorescence Measurement. The GFP fluorescence intensity was determined using a fluorescence spectrophotometer (F-4500; Hitachi, Japan) with a bandwidth of 5 nm, an excitation wavelength of 488 nm, and an emission wavelength of 510 nm. Cells were diluted to an OD_{600} of 1.0 by using a PBS buffer (pH 7.5) before fluorescence was measured. The fluorescence signal of the untransformed cells diluted to an OD_{600} of 1.0 was set as the background level and was subtracted from the overall fluorescence.

Proteinase Accessibility Assay. Cells were harvested, suspended in a PBS buffer, and adjusted to an OD_{600} of 10. Pronase (4 U/mg, Sigma) was added to a final concentration of 2 mg/mL. Cell suspensions were incubated at 37 °C for 3 h. The residual OPH activity and GFP fluorescence were then determined.

Stability Study of Resting Cultures. For outer membrane integrity analysis, the OPH activity of the resting cell suspension was determined each day over a 2-week duration.[23]

Biodegradation Experiments. The engineered UT26 was precultured in 1/3 LB medium at 30 °C and harvested during log phase. The cultures were centrifuged, and the cell pellets were washed twice with fresh MSM and used as inoculums. Subsequently, 10^6 cells/mL were inoculated into MSM supplemented with 50 mg/L kanamycin, 0.1% glucose, 100 mg/L parathion, and 10 mg/L γ-HCH. Cultures were maintained in 250 mL bottles at 30 °C and 200 rpm on a shaker. The samples without inoculation were kept as controls. The degradation experiments with native UT26 were similarly performed.

Aliquots (1 mL) were removed periodically and extracted twice with 4 mL of ethyl acetate for parathion and hexane for γ-HCH. These extracts were dehydrated with Na_2SO_4 and filtered (0.45 μm). Samples of 1 μL (diluted if necessary) were analyzed using a HP 5890 II GC

equipped with an ECD detector and an OV-1701 GC column. The column, injector, and detector temperatures were maintained at 210, 250, and 300 °C, respectively, with a flow rate of 5.4 mL/min. The concentration was determined by comparing peak areas of the samples to a standard curve.

The soil samples used in this study were never exposed to HCH and OPs before. The soil had a pH of 6.81, and its organic carbon was 5.62 g/kg. Soil samples (5 kg) were sterilized by fumigation with chloroform for 10 days at 30 °C.[25] Subsamples (100 g) of the fumigated and nonfumigated soils were treated under aseptic condition with parathion (100 mg/kg) and γ-HCH (10 mg/kg), respectively. One set of fumigated and nonfumigated soils in triplicate was inoculated with the engineered UT26 (10^6 cells/g), and another set without inoculation was kept as controls. The inoculum was thoroughly mixed into the soils under sterile condition. The soil moisture was adjusted by the addition of distilled water to 40% of its water-holding capacity. The soils were incubated at 30 °C for 15 days in the dark. Extraction of parathion and γ-HCH from the soil was carried out by the methods described in Singh et al.[25] and Bidlan et al.[26] Analysis for parathion and γ-HCH residues was performed by gas chromatography as described above.

RESULTS AND DISCUSSION

Surface Localization of INPNC−OPH−GFP Fusion in *S. japonicum* UT26. Previous studies have shown that truncated INP containing N- and C-domains or even only N-domain can also function as a carrier protein.[6,10] Both InaK from *P. syringae* KCTC1832 and InaV from *P. syringae* INA5 have been used for cell surface display of heterologous proteins.[27,28] Compared to the InaK anchor, the use of the InaV anchor resulted in 100-fold higher OPH activity in *Moraxella* sp.[6]

In the present study, to investigate the feasibility of targeting the OPH−GFP fusion onto the cell surface of *S. japonicum* UT26, the truncated InaV protein (INPNC) was used as a surface-anchoring motif. For heterologous expression of INPNC−OPH−GFP fusion in UT26, the *inpnc−opd−gfp* fusion gene was subcloned into pVLT33, an *E. coli−Pseudomonas* shuttle vector, to generate pNOG33. The broad-host-range vector, pVLT33, is an RSF1010 derivative and, therefore, is able to replicate in a wide variety of Gram-negative bacteria.[29] Expression of INPNC−OPH−GFP fusion was tightly regulated by a *tac* promoter due to the presence of the *lacI*^{q} gene on the plasmid.

To verify the synthesis of INPNC−OPH−GFP fusion in *S. japonicum* UT26, Western blot analysis was performed with whole-cell lysates of UT26 carrying pNOG33 using anti-GFP polyclonal antibody after induction with 0.2 mM IPTG. A specific band at the position of 100 kDa was detected in whole-cell lysates of UT26 carrying pNOG33 (Figure 1, lane 1), which matched well with the molecular mass of the INPNC−OPH−GFP fusion. However, no such protein was detected with the control cells carrying pVLT33 (Figure 1, lane 2). A band at the position of 64 kDa was detected with anti-GFP polyclonal antibody in Western blot, demonstrating that the OPH−GFP fusion was expressed in the control cells carrying pOG33. To assess the distribution of INPNC−OPH−GFP fusion in different subcellular fractions, outer membrane and soluble fractions were probed with anti-GFP polyclonal antibody. The vast majority of target proteins were associated with the outer membrane fraction (Figure 1, lane 5). In contrast, only a small minority of target proteins were detected in soluble fractions (Figure 1, lane 3). Assays for the OPH activity were performed with outer membrane, whole cell, and cell lysate. Over 80% of the OPH activity was detected in the outer membrane fraction. In parallel, >80% of the OPH activity was present on the cell surface as judged from the ratio of whole-cell activity to cell lysate activity.

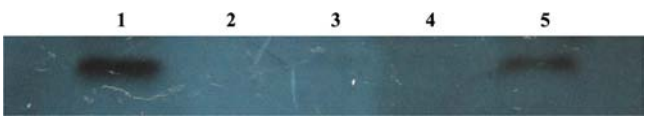

Figure 1. Western blot analysis for subcellular localization of INPNC−OPH−GFP fusion in *S. japonicum* UT26 harboring pNOG33. Lanes: 1, whole-cell lysates; 2, negative control (UT26 harboring pVLT33); 3, soluble fraction; 4, Pronase-digested outer membrane proteins; 5, outer membrane fraction. Anti-GFP polyclonal antibody was used at a 1:1000 dilution.

Proteinases cannot penetrate the outer membrane and, therefore, only surface-exposed proteins can be degraded by proteinases.[5] A proteinase accessibility assay can be used to provide evidence for the surface localization of target proteins. Pronase, which is a mixture of broad-specificity proteinases, is a specific and effective tool for the detection of the cell surface display of GFP.[10,30] After treatment with Pronase for 3 h, an 81% reduction of the fluorescence intensity of GFP was observed in cells carrying pNOG33, which contrasted with the slight reduction (7%) observed in Pronase-treated control cells carrying pOG33. With the Pronase treatment, the OPH activity for cells carrying pNOG33 decreased by 83%, whereas the activity for cells carrying pOG33 dropped only 6%. The fractionated outer membrane samples derived from Pronase-treated cells were probed with anti-GFP polyclonal antibody. As expected, no target proteins were detected in the outer membrane fraction (Figure 1, lane 4) because of the degradation of surface-exposed GFP by Pronase.

Immunolabeling with specific antibodies or antisera is a useful tool to detect surface-exposed proteins.[10] To confirm the presence of INPNC−OPH−GFP fusion on the cell surface, cells were probed with rabbit anti-GFP polyclonal antibody and then fluorescently stained with rhodamine-labeled goat anti-rabbit IgG antibody. Because antibodies cannot diffuse through the outer membrane, specific interactions should only occur with proteins exposed on the cell surface. Under immuno-fluorescence microscopy, orange fluorescence was observed on the cells carrying pNOG33, which indicated that the cell surface of UT26 was covered with antibody−TRITC complex. In contrast, the control cells carrying pOG33 were not immunostained at all. Cells harboring pNOG33 were incubated for 3 h with Pronase and then immunolabeled with anti-GFP polyclonal antibody and rhodamine-conjugated IgG antibody. As a result, Pronase-treated cells were not immunostained completely, indicating that surface-exposed GFP had been removed by Pronase.

Taken together, these results provide strong evidence that the INPNC−OPH−GFP fusion was not only anchored successfully onto the outer membrane but also retained its OPH and fluorescence activity. INP has been shown to possess the ability to target enzymes onto the cell surface of indigenous microbes, such as *Moraxella* sp.[6] and *Pseudomonas* sp.[22] Combining the broad host range vector, pVLT33, with the INP anchoring motif, the surface expression vector, pNOG33, constructed in this study could potentially be expressed in a wide variety of indigenous microbes for the cell surface display of OPH−GFP fusion.

OPH Activity and Fluorescence. The whole-cell OPH activity of UT26 carrying pNOG33 with surface-displayed

OPH was 7-fold higher than that of UT26 carrying pOG33 with an intracellular OPH. The OPH proteins displayed on the cell surface have free access to the extracellular OP pesticides; thus, this enhances whole-cell catalytic activity. Meanwhile, the N-terminus of the OPH protein chain is linked to the outer cell membrane through the INP anchoring motif, so the enzyme is immobilized with enhanced structural stability. Prior to IPTG induction, the OPH activity was not detected and the fluorescence intensity remained at the original background level. The OPH activity and fluorescence intensity increased gradually after induction with 0.2 mM IPTG and reached maxima at 24 h (Table 1). In contrast to the control cells carrying pVLT33, the green fluorescence was observed on the cells carrying pNOG33. Although the fluorescence intensity of GFP was plotted versus the OPH activity, the fluorescence intensity was proportional to the OPH activity (with a correlation coefficient R^2 = 0.996) over the 24 h induction. Thus, GFP can be used as a fusion partner for monitoring the expression and activity of OPH.

Table 1. Time Course of OPH Activity and GFP Fluorescence of Whole Cell[a]

postinduction (h)	OPH activity (U/OD_{600})	fluorescence intensity
0	ND[b]	46 ± 3
6	0.012 ± 0.0020	201 ± 13
12	0.025 ± 0.0021	425 ± 21
18	0.036 ± 0.0024	591 ± 28
24	0.039 ± 0.0025	638 ± 26

[a]Cells harboring pNOG33 were incubated at 30 °C for 24 h after induction with 0.2 mM IPTG. Samples were withdrawn at regular time intervals and measured for the OPH activity and GFP fluorescence of whole cells. Data are the mean ± standard deviations of three replicates. [b]ND, not detected.

Secretion is generally the limiting step for a secretory protein; thus, a high transcription rate may block the translocation pathway and cause growth inhibition of cells.[31] The inhibitory effects of overexpression on the translocation pathway have been reported in previous studies with surface display of GFP.[10,30] Here, effects of different levels of induction on activity and fluorescence were also studied. The expressed INPNC−OPH−GFP was located in the outer membrane fraction when IPTG induction was performed at a concentration of 0.2 mM. However, the fusion proteins produced with induction at higher IPTG concentrations (0.5 and 1 mM) were present only in the soluble fraction (data not shown). In this study, the highest whole-cell OPH activity was obtained at an IPTG concentration of 0.2 mM (Figure 2A). Further induction resulted in a gradual decline in activity. More IPTG caused declines in the OPH activity, probably because of the formation of inclusion body and growth inhibition at increased transcription rates. Unlike the OPH activity, the fluorescence intensity of GFP increased with increasing concentrations of IPTG (Figure 2B). This is due to the fact that fluorescence was minimally affected by the barrier effect of the cell membrane. These results indicate that INPNC−OPH−GFP fusion cannot be efficiently targeted onto cell surfaces under high levels of induction. It is concluded that induction with 0.2 mM IPTG provides an optimal balance between whole-cell activity and fluorescence.

Stability of *S. japonicum* UT26 Displaying INPNC−OPH−GFP Fusion. Two major concerns in surface expression

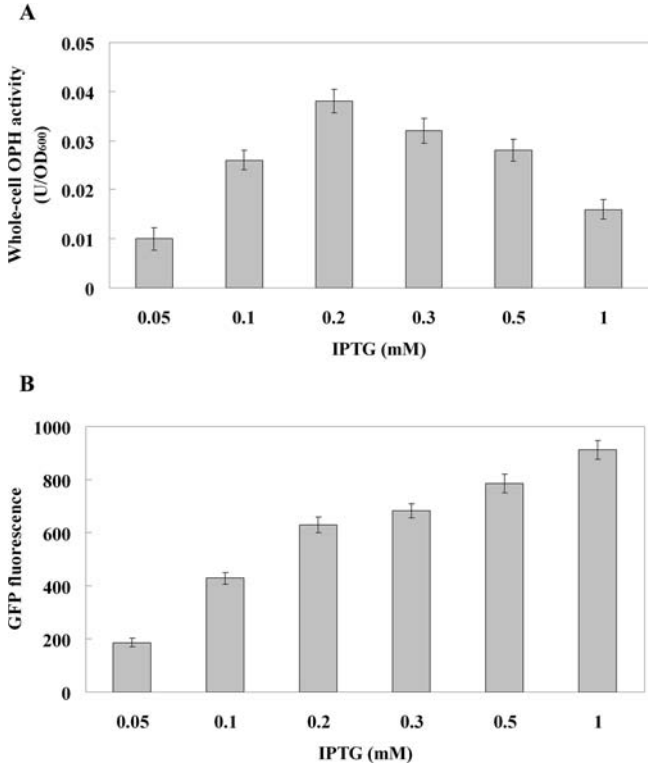

Figure 2. OPH activity (A) and fluorescence intensity (B) of whole cell of *S. japonicum* UT26/pNOG33 under different levels of induction. Data are the mean ± standard deviation of three replicates.

are inhibition of cell growth and instability of outer membrane. To avoid these problems, the size of the inserted gene that can be expressed is usually limited. The INP system looks promising, because it is well suited as a carrier of relatively large inserts. The INP-based system can display proteins as large as 60 kDa.[32] To test whether the surface display of OPH−GFP fusion inhibits cell growth, the growth kinetics of cells carrying pNOG33 or pVLT33 were compared. No growth inhibition was observed for cells expressing INPNC−OPH−GFP fusion. The two cultures reached the same final cell density after 48 h of incubation. To monitor the stability of suspended cultures, whole-cell activity was determined periodically over a 2 week period. The OPH activity of whole cells remained at essentially the original level (0.038 U/OD_{600}) over the duration of 2 weeks. These results show that surface display of OPH−GFP fusion neither disturbed the membrane structure nor caused host growth defects.

Simultaneous Degradation of γ-HCH and Parathion by Engineered UT26. Because parathion is a preferred substrate of OPH, it was used in this study. A higher concentration of parathion and γ-HCH inhibits the cell growth of strain UT26; therefore, an optimal concentration (100 mg/L parathion or 10 mg/L γ-HCH) was used in the biodegradation tests. To determine the rates of parathion and γ-HCH degradation by UT26, the engineered UT26 or wild-type UT26 was inoculated into the MSM containing 100 mg/L parathion and 10 mg/L γ-HCH. Aliquots (1 mL) were removed periodically, extracted, and analyzed by GC-ECD. As shown in Figure 3, the engineered UT26 could degrade γ-HCH as fast as wild-type UT26, indicating that that surface display of INPNC−OPH−GFP fusion did not influence the intrinsic γ-HCH degradation capabilities of wild-type UT26.

dx.doi.org/10.1021/jf304976h | J. Agric. Food Chem. 2013, 61, 1328−1334

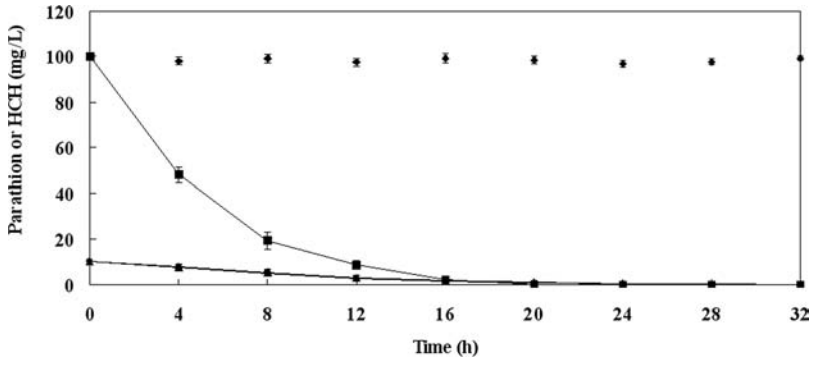

Figure 3. Biodegradation of γ-HCH and parathion by engineered UT26 and wild-type UT26 at an initial rate of 10^6 cells/mL in MSM supplemented with 0.1% glucose containing 10 mg/L γ-HCH and 100 mg/L parathion at 30 °C (▲, degradation of γ-HCH by engineered UT26; ■, degradation of parathion by engineered UT26; ●, degradation of γ-HCH by wild-type UT26; ◆, degradation of parathion by wild-type UT26). Data are the mean ± standard deviation of three replicates.

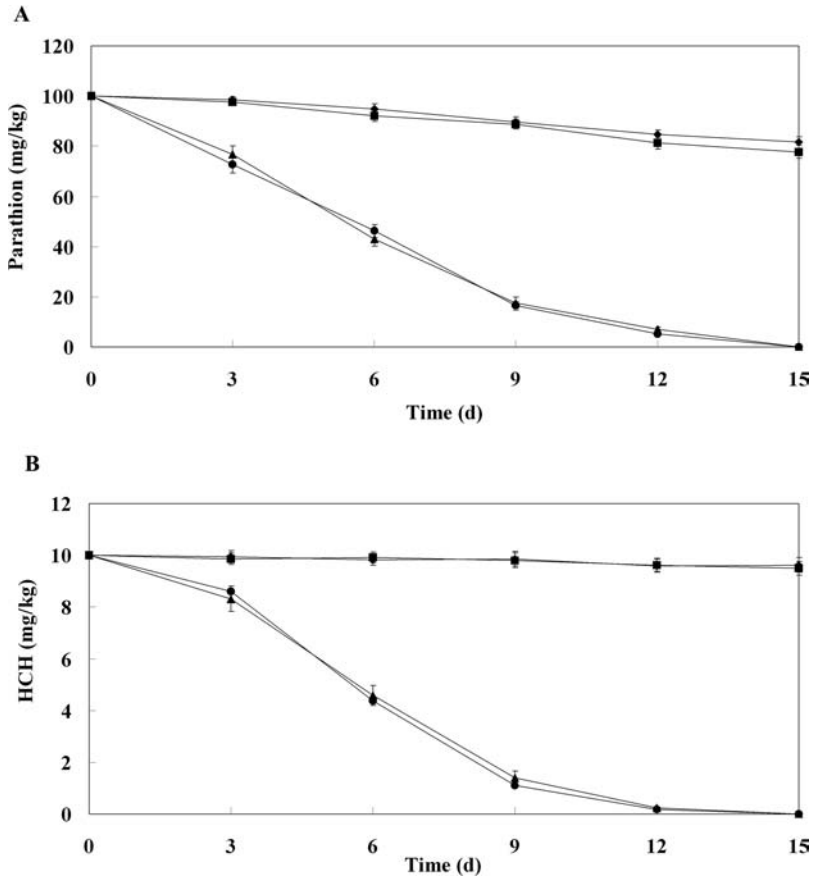

Figure 4. Simultaneous degradation of parathion (A) and γ-HCH (B) by engineered UT26 at an initial rate of 10^6 cells/g in soil containing 100 mg/kg parathion and 10 mg/kg γ-HCH at 30 °C (●, fumigated soil inoculated; ▲, nonfumigated soil inoculated; ◆, fumigated soil uninoculated; ■, nonfumigated soil uninoculated). Data are the mean ± standard deviation of three replicates.

The γ-HCH (10 mg/L) was completely degraded by the engineered UT26 and wild-type UT26 within 32 h. Parathion (100 mg/L) was completely degraded by the engineered UT26 via hydrolysis of the phosphotriester bond in 24 h. In contrast, the concentration of parathion almost did not change in the culture of wild-type UT26, which indicates that the engineered UT26 was endowed with OP degradation capabilities by the heterologous expression of OPH. These results indicate that the engineered UT26 can be used for the cleanup of a mixture of γ-HCH and OP pesticides in environments.

To determine whether the engineered UT26 can thrive and effectively degrade pesticides in soil in the presence of the indigenous microbe populations, fumigated and nonfumigated soils were inoculated with the engineered UT26 at the rate of 10^6 cells/g. Both parathion (100 mg/kg) and γ-HCH (10 mg/kg) could be degraded completely within 15 days in fumigated and nonfumigated soil samples with inoculation (Figure 4). Degradation rates of both pesticides in fumigated soils with inoculation were similar to those of nonfumigated soils. In contrast, only 22% of parathion and 5% of γ-HCH were degraded in control soils without inoculation in 15 day

incubation studies, most likely due to the occurrence of abiotic degradation processes.

After incubation for 15 days, samples from the nonfumigated soils were spread on LB agar plates containing 0.2 mM IPTG, 50 μg/mL kanamycin, and 100 mg/L parathion. Bacterial colonies that developed yellow zones because of the formation of *p*-nitrophenol were isolated and purified. The isolates were identified as *S. japonicum* UT26 by sequencing their 16S rRNA gene. We isolated the same size of plasmid as pNOG33 from the isolates, and the *opd* gene was amplified by PCR from the plasmids. Moreover, all isolates could degrade γ-HCH at the same rate as the strain UT26. The engineered UT26 could be isolated from the nonfumigated soils, which suggests that the inoculated strain UT26 was truly responsible for the observed degradation of parathion and γ-HCH. The *gfp* gene was identified by PCR from all isolates, and the GFP-marked strains emitted green fluorescence under fluorescence microscope, suggesting that GFP is a powerful real-time monitoring tool for the visualization of the engineered UT26 during bioremediation.

The present studies on laboratory-scale soil bioremediation highlight the potential of the engineered UT26 for the removal of HCH and OP residues in the natural environment. In practical field-scale bioremediation, the effectiveness depends on many factors, that is, the degrading capability of the strain, the adaptability of the strain to the fluctuating environmental conditions, competition with indigenous microbial populations, and the bioavailability of contaminants.[25,26] The application of this strain in bioremediation technologies is currently under investigation.

In most situations, it is typically the case that a variety of contaminants exist at a single site. This requires such a strain able to deal with a variety of different contaminants at the same time. In this study, we functionally displayed an INPNC−OPH−GFP fusion on the cell surface of γ-HCH-degrading *S. japonicum* UT26 using an INP anchoring motif. The engineered strain with enhanced OPH activity can be used as a whole-cell biocatalyst, and its activity can be easily monitored by fluorescence. Surface display of the fusion protein had no negative effect on cell growth and outer membrane integrity. The engineered strain was endowed with the capability to simultaneously degrade γ-HCH and OPs, which highlights the enormous potential of the strain for the bioremediation of soil contaminated with multiple pesticides.

AUTHOR INFORMATION

Corresponding Author

*(X.C.) Phone/fax: 86-24-62202232. E-mail: xiangyucao@yahoo.cn. (C.S.) Phone/fax: 86-22-23503866. E-mail: songcj@nankai.edu.cn.

Author Contributions

‖C.Y. and R.L. contributed equally to this work.

Funding

We gratefully acknowledge financial support from the National Key Basic Research Program of China (973 Program, No. 2012CB725204), the National Science Foundation of China (No. 31240005), and a Nankai University Youth Teacher Grant (No. 65012411).

Notes

The authors declare no competing financial interest.

REFERENCES

(1) Jin, F.; Wang, J.; Shao, H.; Jin, M. Pesticide use and residue control in China. *J. Pestic. Sci.* **2010**, *35*, 138−142.

(2) Singh, B. K.; Walker, A. Microbial degradation of organophosphorus compounds. *FEMS Microbiol. Rev.* **2006**, *30*, 428−471.

(3) Singh, B. K. Organophosphorus-degrading bacteria: ecology and industrial applications. *Nat. Rev. Microbiol.* **2009**, *7*, 156−164.

(4) Sogorb, M. A.; Vilanova, E.; Carrera, V. Future application of phosphotriesterases in the prophylaxis and treatment of organophosphorus insecticide and nerve agent poisoning. *Toxicol. Lett.* **2004**, *151*, 219−233.

(5) Richins, R. D.; Kaneva, I.; Mulchandani, A.; Chen, W. Biodegradation of organophosphorus pesticides by surface-expressed organophosphorus hydrolase. *Nat. Biotechnol.* **1997**, *15*, 984−987.

(6) Shimazu, M.; Mulchandani, A.; Chen, W. Simultaneous degradation of organophosphorus pesticides and *p*-nitrophenol by a genetically engineered *Moraxella* sp. with surface-expressed organophosphorus hydrolase. *Biotechnol. Bioeng.* **2001**, *76*, 318−324.

(7) Li, C.; Zhu, Y.; Benz, I.; Schmidt, M. A.; Chen, W.; Mulchandani, A.; Qiao, C. Presentation of functional organophosphorus hydrolase fusions on the surface of *Escherichia coli* by the AIDA-I autotransporter pathway. *Biotechnol. Bioeng.* **2008**, *99*, 485−490.

(8) Kozloff, L. M.; Turner, M. A.; Arellano, F. Formation of bacterial membrane ice-nucleation lipoglycoprotein complexes. *J. Bacteriol.* **1991**, *173*, 6528−6536.

(9) Wolber, P. K. Bacterial ice nucleation. *Adv. Microb. Physiol.* **1993**, *34*, 203−237.

(10) Li, L.; Kang, D. G.; Cha, H. J. Functional display of foreign protein on surface of *Escherichia coli* using N-terminal domain of ice nucleation protein. *Biotechnol. Bioeng.* **2004**, *85*, 214−221.

(11) Nagata, Y.; Endo, R.; Ito, M.; Ohtsubo, Y.; Tsuda, M. Aerobic degradation of lindane (γ-hexachlorocyclohexane) in bacteria and its biochemical and molecular basis. *Appl. Microbiol. Biotechnol.* **2007**, *76*, 741−752.

(12) Zhang, G.; Parker, A.; House, A.; Mai, B.; Li, X.; Kang, Y.; Wang, Z. Sedimentary records of DDT and HCH in the Pearl River Delta, South China. *Environ. Sci. Technol.* **2002**, *36*, 3671−3677.

(13) Qiu, X.; Zhu, T.; Li, J.; Pan, H.; Li, Q.; Miao, G.; Gong, J. Organochlorine pesticides in the air around the Taihu Lake, China. *Environ. Sci. Technol.* **2004**, *38*, 1368−1374.

(14) Senoo, K.; Wada, H. Isolation and identification of an aerobic γ-HCH decomposing bacterium from soil. *Soil Sci. Plant Nutr.* **1989**, *35*, 79−87.

(15) Kumari, R.; Subudhi, S.; Suar, M.; Dhingra, G.; Raina, V.; Dogra, C.; Lal, S.; van der Meer, J. R.; Holliger, C.; Lal, R. Cloning and characterization of *lin* genes responsible for the degradation of hexachlorocyclohexane isomers by *Sphingomonas paucimobilis* strain B90. *Appl. Environ. Microbiol.* **2002**, *68*, 6021−6028.

(16) Ceremonie, H.; Boubakri, H.; Mavingui, P.; Simonet, P.; Vogel, T. M. Plasmid-encoded gamma-hexachlorocyclohexane degradation genes and insertion sequences in *Sphingobium francense* (ex-*Sphingomonas paucimobilis* Sp+). *FEMS Microbiol. Lett.* **2006**, *257*, 243−252.

(17) Imai, R.; Nagata, Y.; Senoo, K.; Wada, H.; Fukuda, M.; Takagi, M.; Yano, K. Dehydrochlorination of γ-hexachlorocyclohexane (γ-BHC) by γ-BHC-assimilating *Pseudomonas paucimobilis*. *Agric. Biol. Chem.* **1989**, *53*, 2015−2017.

(18) Lal, R.; Pandey, G.; Sharma, P.; Kumari, K.; Malhotra, S.; Pandey, R.; Raina, V.; Kohler, H. P.; Holliger, C.; Jackson, C.; Oakeshott, J. G. Biochemistry of microbial degradation of hexachlorocyclohexane and prospects for bioremediation. *Microbiol. Mol. Biol. Rev.* **2010**, *74*, 58−80.

(19) Chalfie, M.; Tu, Y.; Euskirchen, G.; Ward, W. W.; Prasher, D. C. Green fluorescent protein as a marker for gene expression. *Science* **1994**, *263*, 802−805.

(20) Cormack, B. P.; Valdivia, R. H.; Falkow, S. FACS-optimized mutants of the green fluorescent protein (GFP). *Gene* **1996**, *173*, 33−38.

(21) Sambrook, J.; Russel, D. W. *Molecular Cloning: A Laboratory Manual*, 3rd ed.; Cold Spring Harbor Laboratory Press: Cold Spring Harbor, NY, 2001.
(22) Lei, Y.; Mulchandani, A.; Chen, W. Improved degradation of organophosphorus nerve agents and *p*-nitrophenol by *Pseudomonas putida* JS444 with surface-expressed organophosphorus hydrolase. *Biotechnol. Prog.* **2005**, *21*, 678−681.
(23) Yuan, Y.; Yang, C.; Song, C.; Jiang, H.; Mulchandani, A.; Qiao, C. Anchorage of GFP fusion on the cell surface of *Pseudomonas putida*. *Biodegradation* **2011**, *22*, 51−61.
(24) Grag, B.; Dogra, R. C.; Sharma, P. K. High-efficiency transformation of *Rhizobiumleguminosarum* by electroporation. *Appl. Environ. Microbiol.* **1999**, *65*, 2802−2804.
(25) Singh, B. K.; Walker, A.; Morgan, J. A. W.; Wright, D. J. Biodegradation of chlorpyrifos by enterobacter strain B-14 and its use in bioremediation of contaminated soils. *Appl. Environ. Microbiol.* **2004**, *70*, 4855−4863.
(26) Bidlan, R.; Afsar, M.; Manonmami, H. K. Bioremediation of HCH-contaminated soil: elimination of inhibitory effects of the insecticide on radish and green gram seed germination. *Chemosphere* **2004**, *56*, 803−811.
(27) Schmid, D.; Pridmore, D.; Capitani, G.; Battistuta, R.; Nesser, J. R.; Jann, A. Molecular organization of the ice nucleation protein InaV from *Pseudomonas syringae*. *FEBS Lett.* **1997**, *414*, 590−594.
(28) Jung, H. C.; Lebeault, J. M.; Pan, J. G. Surface display of *Zymomonas mobilis* levansucrase by using the ice-nucleation protein of *Pseudomonas syringae*. *Nat. Biotechnol.* **1998**, *16*, 576−580.
(29) de Lorenzo, V.; Eltis, L.; Kessler, B.; Timmis, K. N. Analysis of *Pseudomonas* gene products using *lacI*^{q}/*Ptrp-lac* plasmids and transposons that confer conditional phenotypes. *Gene* **1993**, *123*, 17−24.
(30) Shi, H.; Su, W. W. Display of green fluorescent protein on *Escherichia coli* cell surface. *Enzyme Microb. Technol.* **2001**, *28*, 25−34.
(31) Rodrigue, A.; Chanal, A.; Beck, K.; Muller, M.; Wu, L. F. Co-translocation of a periplasmic enzyme complex by a hitchhiker mechanism through the bacterial Tat pathway. *J. Biol. Chem.* **1999**, *274*, 13223−13228.
(32) Lee, S. Y.; Choi, J. H.; Xu, Z. Microbial cell-surface display. *Trends Biotechnol.* **2003**, *21*, 45−52.